Figure S1: Analysis of REST levels in normal human mammary tissue and human breast cancer. Related to Figure 1.

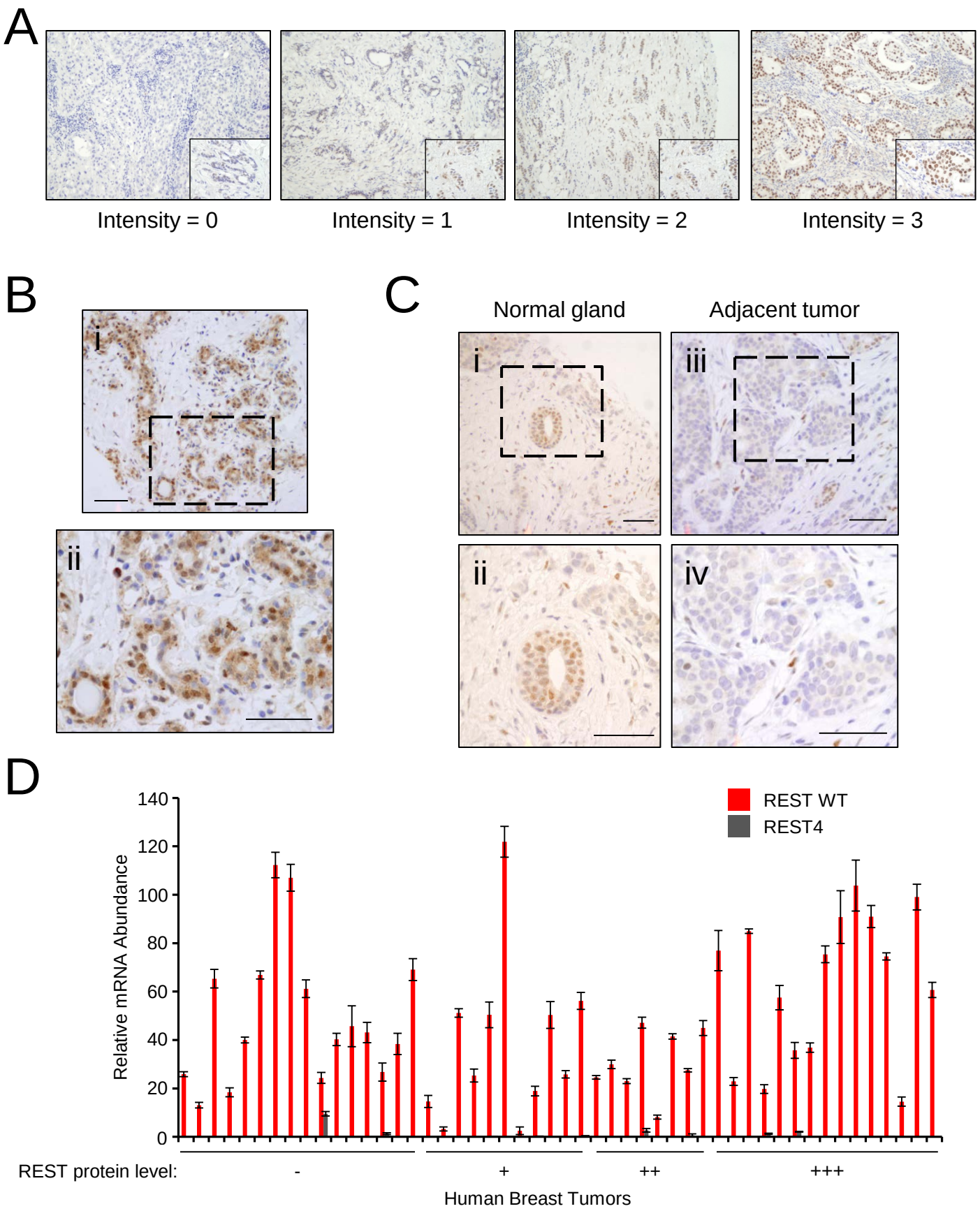

Figure S1. Immunohistochemical analysis of REST protein levels in human breast cancer.

A. Analysis of REST protein expression in human breast cancer. REST protein expression was examined in 185 primary human breast tumor samples via immunohistochemistry. Images representative of the REST protein expression observed with the associated pathology score.

B. Analysis of REST protein levels in normal human mammary tissue. REST protein expression was examined in a panel of normal human mammary tissue samples (8 independent donors). Representative images are shown. Scale bar = 50um

C. REST protein is expressed in normal mammary gland adjacent to tumor tissue. Representative images from a REST-negative TNBC (IHC score = 0) with an adjacent REST-positive normal mammary gland. Scale bar = 50um

D. The alternative splice variant, REST4, is not expressed in human breast cancer. Full-length and REST4 specific qRT-PCR was performed on a subset (n=50) of the tumors analyzed in A. Data presented as mean +/- SE.

Figure S2: Depletion of PLK1, SCYL1 and TEX14 increases REST protein half-life. Related to Figure 2 and Figure 3.

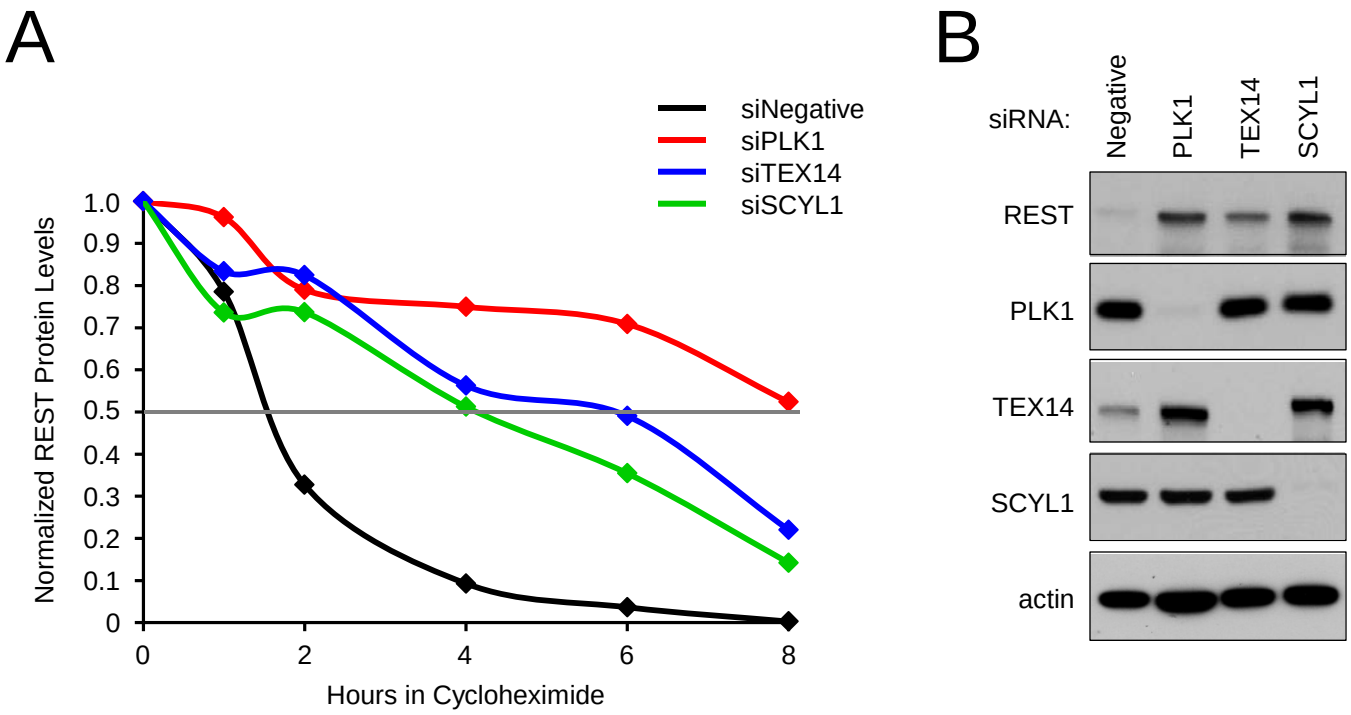

Figure S2. Depletion of PLK1, SCYL1 and TEX14 increases REST half-life.
A. REST protein half-life increases after PLK1, SCYL1 and TEX14 depletion. 293T cells transfected with the indicated siRNAs were treated with cycloheximide for the indicated times. REST protein levels were analyzed by western blot and densitometry was performed. REST protein levels were normalized to actin (loading control).
B. PLK1, SCYL1 and TEX14 depletion. 293T cells were transfected with the indicated siRNAs and western blot analysis was performed as specified.

Figure S3: REST interacts with SCYL1, TEX14 and PLK1 in human TNBC cells. Related to Figure 2 and Figure 3.

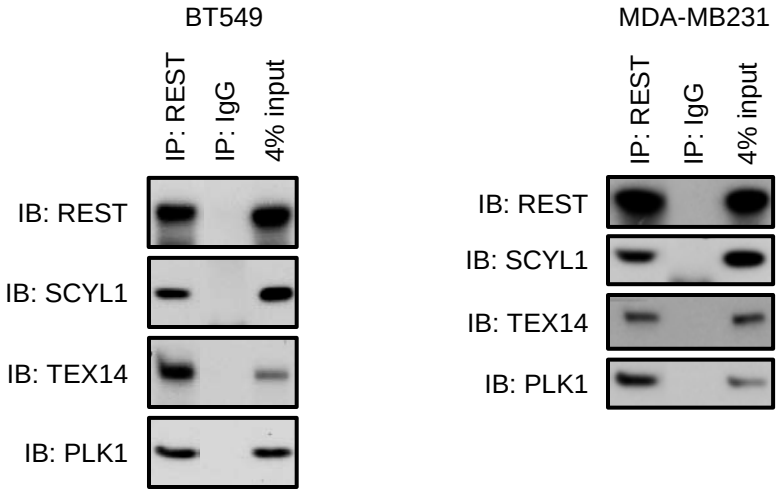

Figure S3. REST interacts with SCYL1, TEX14 and PLK1 in human TNBC cells. Endogenous REST protein was immunoprecipitated from BT549 and MDA-MB231 human TNBC cells and analyzed by western blot as indicated.

Figure S4: PLK1 phosphorylates the REST degron. Related to Figure 2.

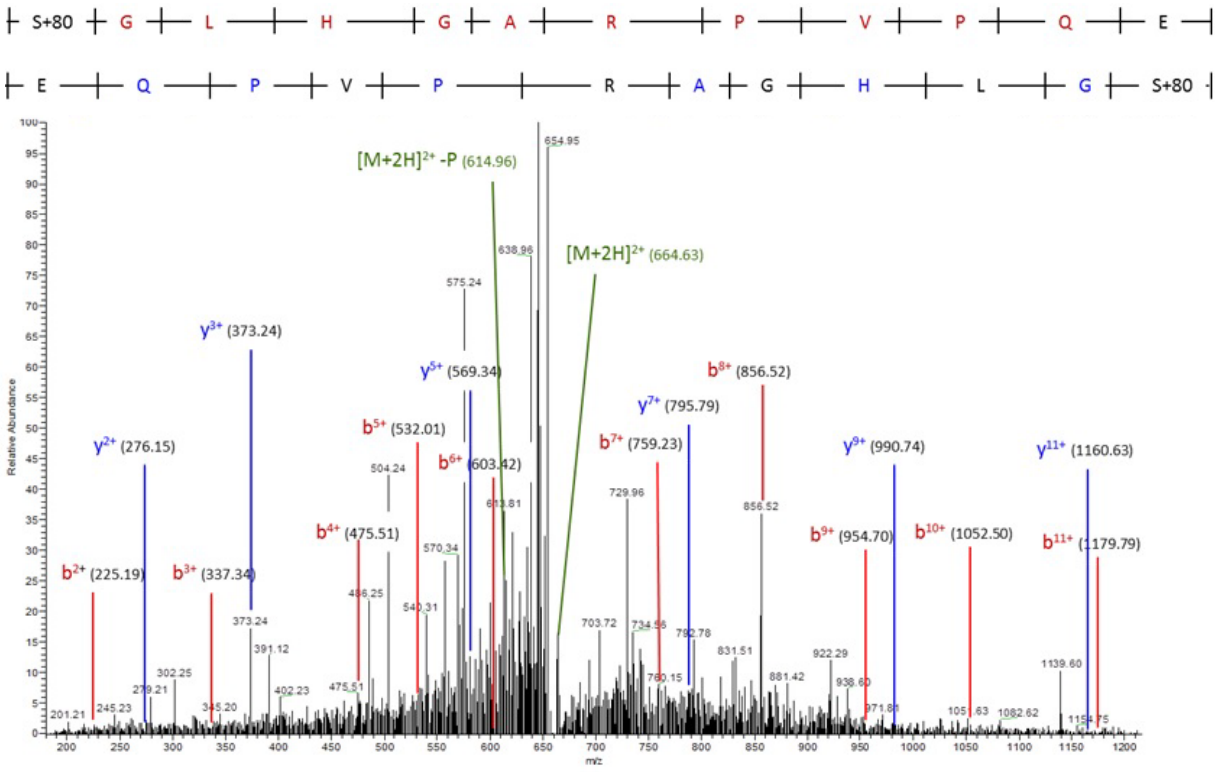

Figure S4. PLK1 phosphorylates the REST degron.
REST is phosphorylated on serine 1030 by PLK1. Mass spectrometry was performed to identify phosphorylated sites within the C-terminus of REST. Ion fragmentation spectra are shown for the phosphorylated peptide. Phosphorylated residue corresponds to serine-1030 in the REST protein.

Figure S5: RNAi-mediated depletion of SCYL1 and TEX14. Related to Figure 3.

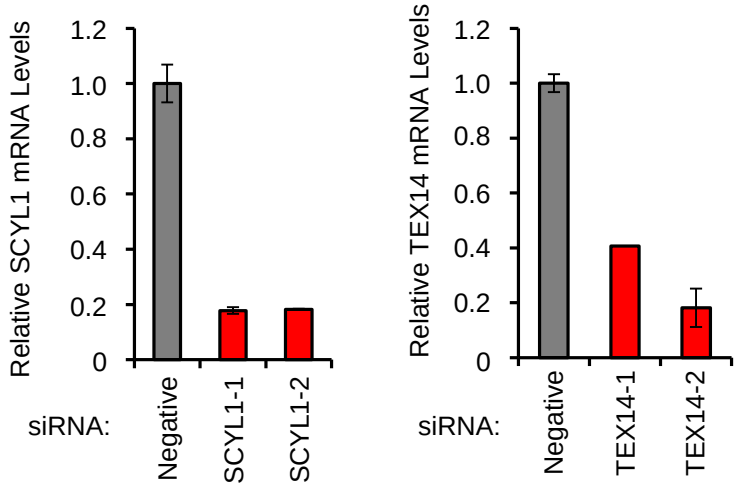

Figure S5. RNAi-mediated depletion of SCYL1 and TEX14.
SCYL1 (left) and TEX14 (right) mRNA levels were determined by qRT-PCR in 293T cells transfected with the indicated siRNAs. Data present mean +/- SE.

Figure S6: SCYL1 is required for the PLK1-REST interaction in human TNBC cells. Related to Figure 3.

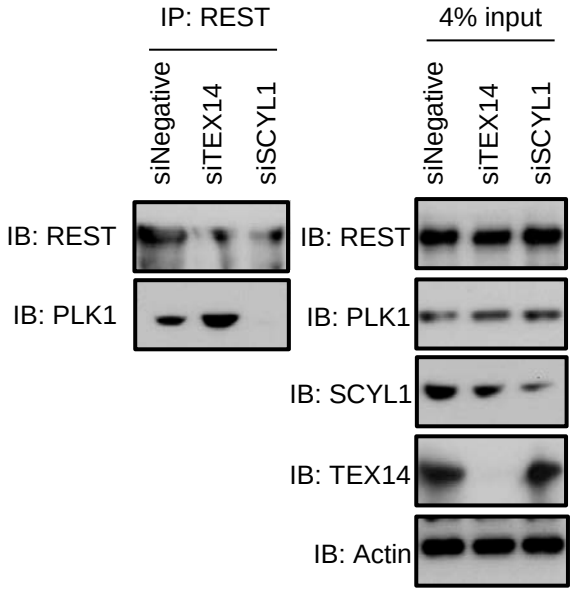

Figure S6. SCYL1 is required for the PLK1-REST interaction in human TNBC cells. Endogenous REST was immunoprecipitated from MLN4924-treated MDA-MB231 TNBC cells transfected with the indicated siRNAs and analyzed via western blot for the specified proteins.

Figure S7: STP axis components are amplified and overexpressed in human breast cancers. Related to Figure 4.

A

	Amplifications (%)	Amplifications <10MB (%)
TEX14	9.3	5.9
SCYL1	2.3	2.2
PLK1	9.6	0.9

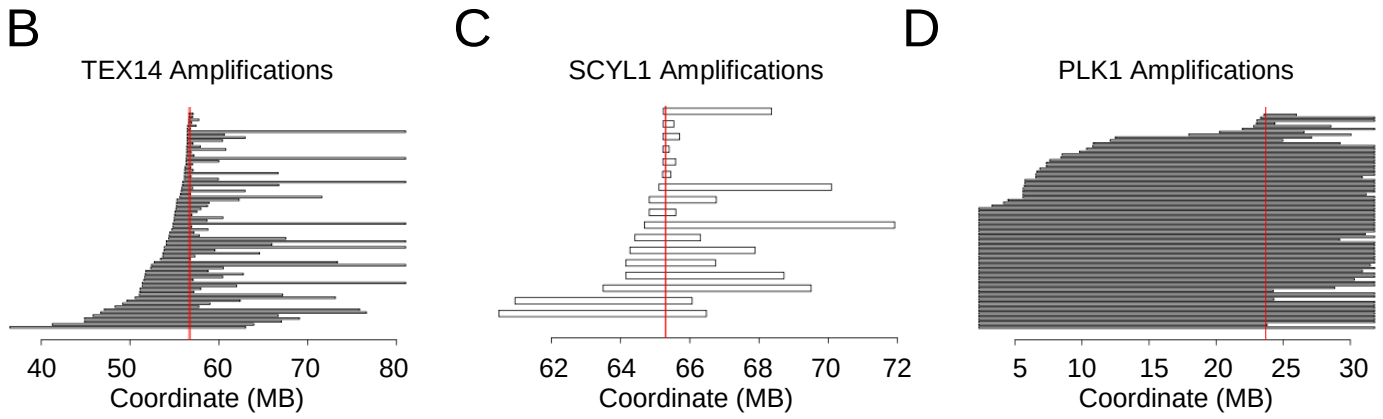

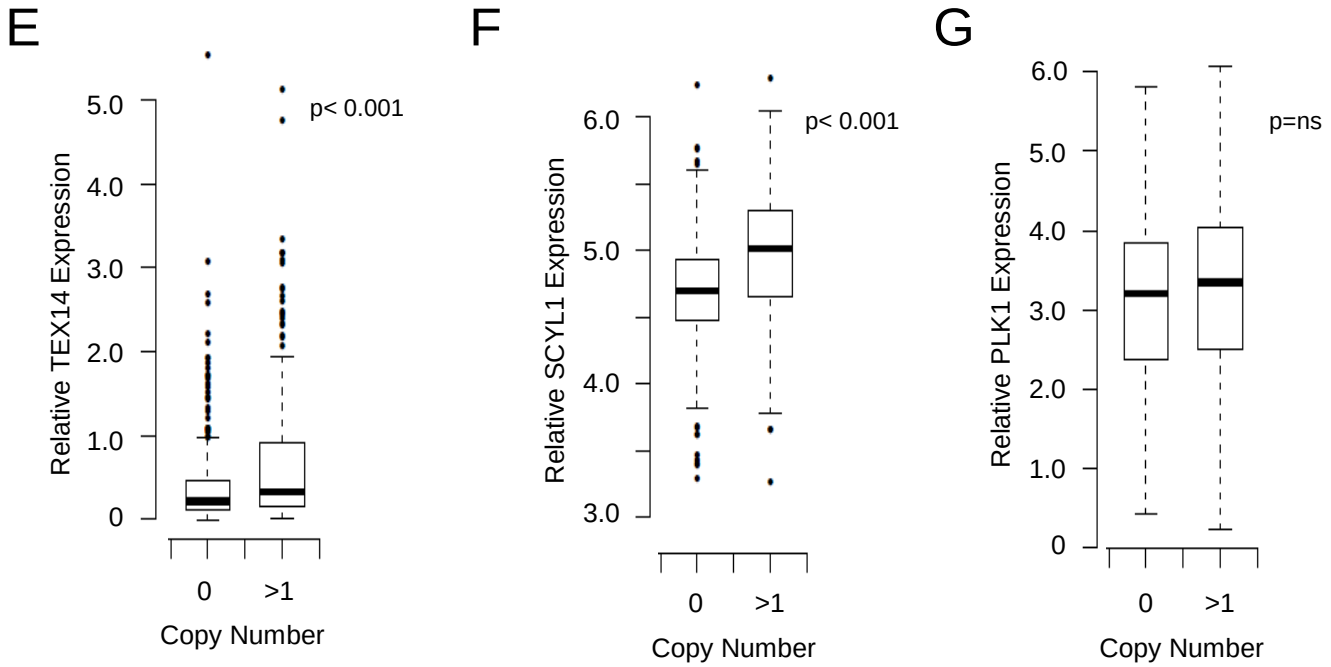

Figure S7. STP axis components are amplifed in human breast cancers.
A. The STP axis is frequently amplified in human breast cancer. The frequency of amplifications in the SCYL1, TEX14 and PLK1 loci in the TCGA breast cancer cohort (n=773). Frequency of amplifications < 10 MB is shown to the right.
B. TEX14 is amplified in human breast cancers. Amplicons (less than 30MB) containing the TEX14 locus (red line) are represented by the rectangles.
C. SCYL1 is amplified in human breast cancers. Amplicons (less than 30MB) containing the SCYL1 locus (red line) are represented by the rectangles.
D. PLK1 is amplified in human breast cancers. Amplicons (less than 30MB) containing the PLK1 locus (red line) are represented by the rectangles.
E. TEX14 mRNA expression correlates with TEX14 amplification. TEX14 mRNA expression level from tumors with TEX14 copy-number neutral (left) or TEX14-gains (right). The median TEX14 expression level is represented by the solid line. The boxes represent the 25^{th} to 75^{th} percentiles. Error bars represent 95% confidence interval. Outliers are represented as circles.
F. SCYL1 mRNA expression correlates with SCYL1 amplification. SCYL1 mRNA expression level from tumors with SCYL1 copy-number neutral (left) or SCYL1-gains (right). The median SCYL1 expression level is represented by the solid line. The boxes represent the 25^{th} to 75^{th} percentiles. Error bars represent 95% confidence interval. Outliers are represented as circles.
G. PLK1 mRNA expression does not correlate with PLK1 copy number. PLK1 mRNA expression level from tumors with PLK1 copy-number neutral (left) or PLK1-gains (right). The median PLK1 expression level is represented by the solid line. The boxes represent the 25^{th} to 75^{th} percentiles. Error bars represent 95% confidence interval. Outliers are represented as circles.

Supplemental Experimental Procedures

Vectors and Virus Production

Individual pGIPZ shRNAs targeting firefly luciferase (negative), SCYL1 (V3LHS_347640, V2LHS_57900), TEX14 (V3LHS_643746, and previously described (Mondal et al., 2012)) and REST (V2LHS_57045) were from Open Biosystems. For constitutive RNAi, negative control and REST shRNAs were subcloned into MSCV-pM using XhoI and MluI. For inducible RNAi or overexpression experiments, shRNAs or cDNAs were cloned into the pINDUCER lentiviral expression system (Meerbrey et al., 2011). The REST and PLK1 cDNAs were recombined into a retroviral pQCXIN-N-YFP fusion vector (amino acids 1-155 of YFP) and pQCXIN-C-YFP fusion vector (amino acids 156-239 of YFP) for BiFC experiments, respectively. GST-REST fragments were generated by PCR amplifying the sequence of interest and recombining into a GST-tagged expression vector (pDEST27) and REST-S1030A was previously described (Westbrook et al., 2008). FLAG-TEX14 constructs were previously described (Mondal et al., 2012). SCYL1 and TEX14 cDNAs were recombined into pHAGE-CMV-HA and pHR-Sin-CSGN expression vectors for constitutive expression, respectively. Lentiviral and retroviral supernatants were generated by transiently transfecting 293T cells following MIRUS Bio's TransIT 293 protocols and harvested 48 hours after transfection.

Immunoblotting

Cells were lysed in 1x SDS sample buffer (62.5mM Tris-HCl, pH6.8, 10% glycerol, 2% SDS, 2.5% β-mercaptoethanol) and heated at 95C for 12 minutes. The following antibodies were used for western blotting: REST (Millipore 07-579); PLK1 (Santa Cruz sc-17783); SCYL1 (Sigma HPA015015); TEX14 (Mondal et al., 2012); βTRCP (D13F10) (Cell Signalling #4394); vinculin (Sigma V9131); actin (Sigma); GST (Sigma); FLAG (Sigma).

Cell Culture

293T cells, MDA-MB231-LM2 and BT549 breast cancer cells were cultured in DMEM (Gibco) supplemented with 10% fetal bovine serum (FBS). TLM-HMECs were cultured in mammary epithelial growth media (MEGM, Lonza). All cell lines were incubated at 37°C and 5% CO2. Stable cell lines expressing indicated shRNAs or cDNAs were generated by retroviral or lentiviral transduction in the presence of 8ug/mL polybrene followed by selection with appropriate antibiotic resistance markers. For evaluating endogenous REST levels and protein interactions, cells were either aligned in prometaphase by treatment with 20μg/mL monastrol (Sigma) (to enrich for cells with active PLK1), treated with 20μg/mL MG132 (Sigma) (to inhibit the proteasome), 100μg/mL cycloheximide (Sigma) (to inhibit protein synthesis), or 1μM MLN4924 (Selleck) (to inhibit REST degradation) as indicated in individual experiments. PLK1 was inhibited with BI2536 or BI6727 (Selleck) as indicated.

RNA Isolation and qRT-PCR

RNA was isolated using the RNeasy Mini kit (Qiagen). Reverse transcription was performed using the High Capacity RNA-to-cDNA Master Mix (Applied Biosystems) and qPCR was performed using SBYR Green Master Mix (Applied Biosystems) and the associated protocols. To compare mRNA levels of wild-type REST and REST4, Ct values from the human tumor samples were interpolated on a standard curve performed with the following synthesized cDNA oligos.

REST full-length:

ATATGCGTACTCATTCAGGTGAGAAGCCATTTAAATGTGATCAGTGCAGTTATGTGG
CCTCTAATCAACATGAAGTAACCCGCCATGCA.

REST4:

GTACTCATTCAGTGGGGTATGGATACCATTTGGTAATATTTACTAGAGTGTGATCTA

GATGGGTGAGAAGCCATTT.

The following primers were used. The REST4 primers were previously published (Wagoner et al., 2010).

Target	Forward	Reverse
REST	GGAGGAGGAGGGCTGTTTACC	GTCGTTAGGCAGGGCCATT
REST Full-length	CGTACTCATTCAGGTGAGAAG	AACATGAAGTAACCCGCC
REST4	CATTCAGTGGGGTATGGATACC	GTGTGATCTAGATGGGTGAGAAGC
SCYL1	GCTCTGCGGTCTCACTGTAGA	GCTCCGAATGGCCTTGAAG
TEX14	GCGTTATTGGGCCTTAGGAAA	AGCAGCGGTGATTTGGATCT
PLK1	TGATGGCAGCCGTGACCTA	GGCGGTATGTGCGGAAGT
GAPDH	CCTCCCGCTTCGCTCTCT	TGGCGACGCAAAAGAAGAT

Immunohistochemistry of Primary Tumors

A REST immunohistochemical assay (antibody: Millipore 07-579) was optimized and validated on paraffin-embedded cell pellets from human mammary epithelial cells (HMECs) with or without REST-shRNA expression (to confirm depletion of immuno-reactive signal). The specificity of the antibody was also confirmed as a single immuno-reactive species by western analysis on HMECs with a control- or REST-shRNA. REST protein expression was analyzed in a cohort of 185 human invasive breast cancers (purchased from Asterand, plc). ER, PR, and HER2 status were provided by Asterand, plc. and confirmed by independent IHC (I.M.,

unpublished data). Four μm sections of primary tumors were immunostained using standard protocols. Briefly, antigen retrieval was performed by heating in 0.1M Tris–HCl buffer (pH 9.0). Sections were incubated with REST primary antibody at a dilution of 1:100. Slides were incubated with secondary biotinylated antibody and subsequently with streptavidin-peroxidase. The enzyme was visualized after 15 min incubation with diaminobenzidine (DAB). Slides were counterstained with hematoxylin. Positive and negative controls were included in each staining.

REST immunostaining was quantified by a pathologist in a double blind fashion. The cellular intensity of REST staining ("intensity score") and percentage of REST-positive tumor cells ("propensity score") were evaluated for each tumor. REST levels were expressed as the intensity score (0-3) x propensity score (0-100%). For example, a tumor with intensity score of 2.0 and propensity score of 50% is equal to 1.0.

Bimolecular Fluorescence Complementation (BiFC)

N-terminal domain (residues 1–155) of Venus YFP was fused N-terminal to REST (bait). C-terminal domain (residues 156–239) of Venus YFP was fused N-terminal or C-terminal to PLK1 (prey). TLM-HMECs were transduced with retroviruses encoding bait and individual preys as described above. Cell fluorescence was analyzed by flow cytometry in triplicate.

Protein Purification

REST fragments were generated by PCR amplifying the sequence of interest and recombining into pGEX2T for expression in bacteria. REST fragments were expressed with 0.5mM IPTG at 37°C for 3 hours in BL21DE3 gold transformed competent bacterial cells (Agilent). Transformed bacterial cells were frozen as cell pellets at -80°C, thawed and pellets lysed for 20 minutes in 50mM Tris pH 8.0, 250mM KCl, 1mM EDTA, 1% Triton X-100 + protease inhibitors (Roche Complete Protease Inhibitor tablets, Pefablock), 10 mg lysozyme, 10mM $MgCl_2$, 1.5 mg DNase

I, and 12 U/ml benzonase nuclease (Novagen). Lysis was followed by two freeze-thaw cycles. After second thaw, the lysate was clarified by centrifugation at 20,000 rpm for 30 minutes at 4°C. The clarified lysate was then dialyzed for 3 hours 4°C and bound in batch to Glutathione Sepharose 4B (GE Healthcare) overnight at 4°C. The beads were transferred to a column, and washed with 50 ml binding/wash buffer followed by high salt wash buffer with 3 M NaCl. The beads were washed with 75 ml low salt wash/elution buffer (200 mM NaCl) and equilibrated with low salt wash/elution buffer with 2.5mM $CaCl_2$. The beads were then incubated for 4 hours at room temperature in elution buffer with 2.5 mM $CaCl_2$ and 32 U thrombin and cleavage was stopped with 1 mM Pefablock. Eluted protein was concentrated by ultracentrifugation with an Amicon 10,000 molecular weight cut-off centrifugal filtration device (Millipore). Immunoblotting with a REST antibody (Millipore) was done to confirm the purity of the REST fragments.

In vitro Kinase Assays and Mass Spectrometry

Active PLK1 (Millipore) was incubated with ATP [γ^{32}P] and purified REST WT or Δdegron at 30°C for 15 minutes in kinase reaction buffer (20 mM Tris, pH 7.5, 1 mM EGTA, 2 mM $MgCl_2$, 1 mM NaF, 0.1 mM Na_3VO_4, and 50 μM ATP). The reaction was stopped by incubating at 70°C for 10 minutes. SDS-PAGE and audioradiography was performed. Quantitation was performed by imaging on a Phosphorimager.

The nLC-MS/MS analysis and phosphorylation site identification was carried-out as previously reported with minor modifications (Jung et al., 2008). *In vitro* kinase reaction mixture were boiled with Laemmli buffer, and subjected to SDS-PAGE. Coomassie brilliant blue stained REST protein contained gel pieces were destained and subjected to in-gel digestion using 100 ng Glu-C (Promega) in 50 mM NH4HCO3, pH 8.5, for 2 hours. Peptides were then extracted with

acetonitrile, vacuum dried. The peptide then dissolved in 5µl of loading solution (0.2% formic acid) and subjected to nanoflow LC-MS/MS analysis with a nano-LC1000 (Thermo Scientific) coupled to Orbitrap Elite™ (Thermo Scientific) mass spectrometer. The peptides were loaded onto an in-housed Reprosil-Pur Basic C18 (3 µm, Dr.Maisch GmbH, Germany) trap column which was 2 cm X 75 um size. Then the trap column was washed with loading solution and switched in-line with an in-housed 100 mm x 75 um column packed with Reprosil-Pur Basic C18 equilibrated in 0.1% formic acid/water. The peptides were separated with a 45 min continuous gradient of 0-10% acetonitrile/0.1% formic acid at a flow rate of 450nl/min. Separated peptides were directly electro-sprayed into LTQ Orbitrap Velos mass spectrometer. The Orbitrap Elite instrument was operated in the data-dependant mode acquiring fragmentation spectra of the top 75 strongest ions and under direct control of Xcalibur software (Thermo Scientific). Obtained MS/MS spectra were searched against target-decoy Human refseq database in Proteome Discoverer 1.4 interface (Thermo Fisher) with Mascot algorithm (Mascot 2.4, Matrix Science). Variable modification of Phosphorylation (Serine, Threonine, and Tyrosine) and Oxidation (Methionine) was allowed. The precursor mass tolerance was confined within 10 ppm with fragment mass tolerance of 0.6 dalton and a maximum of two missed cleavage allowed. Assigned peptides were filtered with 5% false discover rate (FDR) and subject to manual verifications.

Immunoprecipitation

Cell pellets were lysed in 2.5% SDS, 0.5% deoxycholate and 0.5% NP40 and diluted with 900 µl of immunoprecipitation (IP) buffer (190 mM NaCl, 50 mM Tris HCl (pH 7.4), 6 mM EDTA and 2.5% NP40). Lysates were incubated at 4°C overnight with primary antibodies and then with either Protein-A or Protein-G (Roche) beads at 4°C for 2 hours. Beads were washed with NETN

(or IP) buffer and presoaked with 5% BSA before adding to the IPs. Immunoprecipitated proteins were washed 4-6 times with IP buffer and then lysed in Laemmli sample buffer (+ 5% beta-ME). IP or whole cell lysates were run on SDS-PAGE and immunoblotted with various primary antibodies and secondary antibodies conjugated to horseradish peroxidase. Signals were visualized using SuperSignal West Pico Chemiluminescent Substrate (Pierce).

Tumorigenicity and Metastasis Assays

For mixed population experiments, MDA-MB231-LM2 breast cancer cells were individually transduced with pINDUCER14-shSCYL1 and pINDUCER14-shTEX14 (combined) or pINDUCER14 negative control shRNAs at an M.O.I. of 1.5. The individual populations were mixed *in vitro* at equal ratios and expanded for injection. 3×10^6 or 2×10^5 mixed population cells were injected subcutaneously into the flank or into the lateral tail vein of female athymic nude Foxn1-nu mice (Harlan Labs), respectively. The mice were maintained on either sucrose water (-dox), or sucrose water with 2mg/mL dox (+dox). Tumor volume was measured with calipers over time. Lung metastatic progression was monitored and quantified using noninvasive bioluminescence as previously described (Minn et al., 2005).When the tumors reached $1000mm^3$ or the total luminescent flux reach 1×10^9, tumors or lungs were harvested and genomic DNA was harvested using the Qiagen DNA mini kit. qPCR for each barcode was performed with Taqman Fast Master Mix (Applied Biosystems) using the recommend protocol and the following primers and probes. Experimental target Ct values were normalized to the tRFP Ct values (tRFP is present in all pINDUCER-proviruses).

Target	Forward	Probe	Reverse
SCYL1-12	CGGCCGGCCATTGTT	TCGCGTTTACCCCTTG	CACAAAGACCCAAAGACCGACTA
tRFP	TCAAGGAGGCCGACAAAGAG	CCTACGTCGAGCAGCA	GTACTTGGCCACAGCCATCTC

Statistical analysis of the RDR screen (siRNA and gene level analysis)

siRNA level values were available for both mRFP-REST and mRFP signal intensities for each siRNA in each replicate. These values were quantile normalized to remove inter-replicate intensity batch effects. Each siRNA was then subjected to analysis of variance and a linear contrast was computed that differenced the average mRFP-REST and mRFP values. The distribution of these values was graphically displayed for analysis of overall character and the location of controls. For gene level analysis, a more complex two-way ANOVA was performed that integrated multiple siRNAs grouped at the level of the gene where siRNA effects as well as replicate observations of mRFP-REST and mRFP were modeled. Those genes with the strongest aggregate contrast between mRFP-REST and mRFP but where mRFP was low were considered to be the best candidates. Gene level p-values for the mRFP-REST contrast were determined.

Statistical analysis of TCGA data

Analysis of gene expression and copy number data analysis were performed on the breast cancer data derived from TCGA resources (Cancer Genome Atlas, 2012). Immunohistochemistry information was obtained by download from the supplemental tables from the original TCGA BRCA publication (Cancer Genome Atlas, 2012). Segmental calls were obtained by download from the TCGA distribution web-portal. Gene expression and copy number GISTIC2 summaries were obtained from the UCSC Cancer genome browser distribution as obtained in November 2012. To perform analysis of CN and gene expression for the STP genes, the raw segmental data were filtered according to both size (30Mb) and magnitude (< -0.2 segmental mean for losses; > 0.5 segmental mean for gains), and all centromere-crossing events were removed.

For subtype analysis of the TCGA samples, we utilized the ER, PR and HER2 data as expressed in the TCGA BRCA paper supplement (Cancer Genome Atlas, 2012). We stratified

subjects into disjoint subsets. Those negative for ER, PR and HER2 form the TNBC group. Subjects positive for HER2 form the HER2 group irrespective of the ER/PR status. Subjects negative for HER2 but which are ER/PR positive form the last group (ER+). These groups were used to split the subjects for cross tabulation and box plot analysis of the STP expression data.

STP Expression Signatures

To compute a gene set strongly correlated with STP expression in diverse human samples, we used a standard and accepted "co-expression" analyses. We computed the spearman rank correlation between each STP gene and all other genes profiled in the TCGA breast cancer bulk data download, restricting to samples to those represented in both the gene expression and copy number data. We averaged the correlation of each gene with the three STP genes, and we then selected the subset of genes whose average correlation was in the top 5% from among all genes (n= 792 genes). These genes were then used in a variety of analyses as an "STP signature."

Compendium Survival Analysis

A compendium of breast cancer studies with both outcome data and genome wide gene expression was developed by download from GEO. Eight total studies were considered, including: (Chin et al., 2006; Desmedt et al., 2007; Loi et al., 2007; Minn et al., 2007; Minn et al., 2005; Schmidt et al., 2008; Wang et al., 2005; Zhang et al., 2009). Raw cel file gene expression data from these studies was analyzed using the GCRMA method, and gene annotation data was determined using the Bioconductor annotation for the hgu133a microarray. When multiple probe sets were identified to report on the same gene, the probe set with highest average variance across studies was selected for analysis. Gene set signature based survival analysis was performed by first centering each gene's expression within each study around the study mean and then averaging the within-study centered (mean 0) gene expression values to produce

a score for the gene set for each individual. All survival analysis using these values was performed in R using the Survival analysis package; regressions were performed by the Cox proportional hazard method stratified by study. Subject tertiles were determined by rank ordering the gene expression signature for STP within each study to identify within study percentiles of the scores. Intrinsic subtype information was calculated for each subject in the compendium by computing the spearman rank correlation of the gene expression values of the available PAM50 genes in each individual's expression profile with the PAM50 centroids as described in the original publication. Individuals were assigned to the PAM50 class for which they were most strongly correlated as long as this correlation exceeded a cutoff value which was arbitrarily set at a spearman value of 0.25. Subjects without a maximum correlation exceeding this value were unassigned. In addition to proportional hazard analysis, log rank tests were also performed stratified by study.

Supplemental References

Chin, K., DeVries, S., Fridlyand, J., Spellman, P.T., Roydasgupta, R., Kuo, W.L., Lapuk, A., Neve, R.M., Qian, Z., Ryder, T., *et al.* (2006). Genomic and transcriptional aberrations linked to breast cancer pathophysiologies. Cancer Cell *10*, 529-541.

Desmedt, C., Piette, F., Loi, S., Wang, Y., Lallemand, F., Haibe-Kains, B., Viale, G., Delorenzi, M., Zhang, Y., d'Assignies, M.S., *et al.* (2007). Strong time dependence of the 76-gene prognostic signature for node-negative breast cancer patients in the TRANSBIG multicenter independent validation series. Clin Cancer Res *13*, 3207-3214.

Jung, S.Y., Li, Y., Wang, Y., Chen, Y., Zhao, Y., and Qin, J. (2008). Complications in the assignment of 14 and 28 Da mass shift detected by mass spectrometry as in vivo methylation from endogenous proteins. Anal Chem *80*, 1721-1729.

Loi, S., Haibe-Kains, B., Desmedt, C., Lallemand, F., Tutt, A.M., Gillet, C., Ellis, P., Harris, A., Bergh, J., Foekens, J.A., *et al.* (2007). Definition of clinically distinct molecular subtypes in estrogen receptor-positive breast carcinomas through genomic grade. J Clin Oncol *25*, 1239-1246.

Meerbrey, K.L., Hu, G., Kessler, J.D., Roarty, K., Li, M.Z., Fang, J.E., Herschkowitz, J.I., Burrows, A.E., Ciccia, A., Sun, T., *et al.* (2011). The pINDUCER lentiviral toolkit for inducible RNA interference in vitro and in vivo. Proc Natl Acad Sci U S A *108*, 3665-3670.

Minn, A.J., Gupta, G.P., Padua, D., Bos, P., Nguyen, D.X., Nuyten, D., Kreike, B., Zhang, Y., Wang, Y., Ishwaran, H., *et al.* (2007). Lung metastasis genes couple breast tumor size and metastatic spread. Proc Natl Acad Sci U S A *104*, 6740-6745.

Schmidt, M., Bohm, D., von Torne, C., Steiner, E., Puhl, A., Pilch, H., Lehr, H.A., Hengstler, J.G., Kolbl, H., and Gehrmann, M. (2008). The humoral immune system has a key prognostic impact in node-negative breast cancer. Cancer Res *68*, 5405-5413.

Wang, Y., Klijn, J.G., Zhang, Y., Sieuwerts, A.M., Look, M.P., Yang, F., Talantov, D., Timmermans, M., Meijer-van Gelder, M.E., Yu, J., *et al.* (2005). Gene-expression profiles to predict distant metastasis of lymph-node-negative primary breast cancer. Lancet *365*, 671-679.

Zhang, Y., Sieuwerts, A.M., McGreevy, M., Casey, G., Cufer, T., Paradiso, A., Harbeck, N., Span, P.N., Hicks, D.G., Crowe, J., *et al.* (2009). The 76-gene signature defines high-risk patients that benefit from adjuvant tamoxifen therapy. Breast Cancer Res Treat *116*, 303-309.